

# Thermodynamics of the coupled spin-dimer system $\text{TCuCl}_3$ close to a quantum phase transition

T. Lorenz<sup>a,\*</sup>, S. Stark<sup>a</sup>, O. Heyer<sup>a</sup>, N. Holmann<sup>a</sup>, A. Vasiliev<sup>b</sup>, A. Osawa<sup>c</sup>, H. Tanaka<sup>d</sup>

<sup>a</sup>II. Physikalisches Institut, Universität zu Köln, Zulpicher Str. 77, 50937 Köln, Germany

<sup>b</sup>Department of Low Temperature Physics, Moscow State University, Moscow 119992, Russia

<sup>c</sup>Advanced Science Research Center, Japan Atomic Energy Research Institute, Tokai, Ibaraki 319-1195, Japan

<sup>d</sup>Department of Physics, Tokyo Institute of Technology, Oh-okayama, Meguro-ku, Tokyo 152-8551, Japan

## Abstract

We present thermal expansion, magnetostriction and specific heat  $C_m$  measurements of  $\text{TCuCl}_3$ , which shows a quantum phase transition from a spin-gap phase to a Néel-ordered ground state as a function of magnetic field around  $H_{c0} \approx 4.8 \text{ T}$ . Using Ehrenfest's relation, we find huge pressure dependencies of the spin gap for uniaxial as well as for hydrostatic pressure. For  $T \ll 0$  and  $H \ll H_{c0}$  we observe a diverging Grüneisen parameter  $\Gamma(T) = -C_m/T$ , in qualitative agreement with theoretical predictions. However, the predicted individual temperature dependencies  $\Gamma(T)$  and  $C_m(T)$  are not reproduced by our experimental data.

© 2021 Elsevier B.V. All rights reserved.

ACS: 75.30.Kz; 75.80.+q; 65.40.De

Keywords: low-dimensional magnets; Bose-Einstein condensation; magnetoelastic coupling; Quantum phase transition

## 1. Introduction

Low-dimensional quantum magnets show very rich and fascinating physical properties [1]. As a starting point, one may consider isolated spin-1/2 dimers with an antiferromagnetic coupling  $J$  causing a singlet ground state and an excited triplet state, which are separated by an energy gap  $\Delta = J$ . If such dimers are magnetically coupled to each other, a multitude of different theoretical models can be constructed, depending on the strength and the geometric arrangement of the interdimer coupling(s)  $J^0$ . As a consequence of one (or more) non-zero  $J^0$ , finite dispersion(s) of the triplet state evolve along the respective direction(s) in reciprocal space, i.e., the excited triplets may hop along different directions. Of particular interest are one-dimensional (1D) chains with alternating couplings  $J$  and  $J^0$  between neighboring spins, because of qualitatively different excitation spectra of the alternating ( $J^0 \neq J$ ) and the uniform ( $J^0 = J$ ) chain [2]. Another example of 1D coupled spin dimers is represented by so-called spin-ladders with the couplings  $J_r$  and  $J_k$  along the rungs and legs of the ladder, respectively. The excitation gap of two-leg ladders is finite, while it vanishes for a three-leg spin-ladder [3]. This

difference is easily understood in the limit  $J_r \gg J_k$ , where the two-leg ladder can be viewed as weakly coupled dimers and the three-leg ladder as an effective  $S = 1/2$  chain with uniform chain coupling  $J_k$ . With increasing number of legs, the spin ladders approach the 2D antiferromagnetic square lattice. Another well-studied system of 2D-coupled spin dimers is the 2D Shastry-Sutherland model [4], which can be generated from the 2D square lattice by introducing one additional diagonal coupling  $J_D$  on every second square. The triangular arrangement of one  $J_D$  and two  $J$  causes a strong frustration and for  $J = J_D \approx 0.7$  the product state of singlets on every diagonal is the exact ground state.

The above-mentioned models have been studied very intensively by theoretical as well by experimental physicists during the last decades, since a large number of materials became available which rather well represent various types of these models [1]. Some cuprate examples are: the 2D square lattice realized by the parent compound  $\text{La}_2\text{CuO}_4$  of the High- $T_c$ 's, the spin-Peierls system  $\text{CuGeO}_3$  [5], spin-1/2 chain and ladder compounds, such as  $\text{Sr}_2\text{CuO}_3$  and  $\text{SrCu}_2\text{O}_3$ , respectively, as well as  $\text{Sr}_{14}\text{Cu}_{24}\text{O}_{41}$  containing both, spin chains and spin ladders [6], or the 2D Shastry-Sutherland model which is realized in  $\text{SrCu}_2(\text{BO}_3)_2$  [7].

$\text{TCuCl}_3$  is another quantum spin system which has been intensively studied in recent years [9,10]. From the structural point of view this compound contains a ladder-like

\*Corresponding author.

Email address: lorenz@ph2.uni-koeln.de (T. Lorenz).

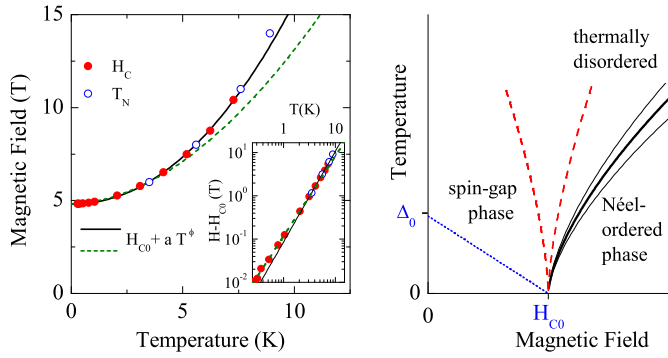


Fig. 1. Left: Phase boundary of  $\text{TlCuCl}_3$  obtained from magnetostriction ( $\bullet$ ) and thermal expansion ( $\circ$ ). The dashed line is a fit of the form  $H_C(T) = H_{C0} + a T^2$  for  $T \leq 2$  K, which yields  $H_{C0} = 4.82$  T and  $a = 1.85$ , while the solid line is a fit up to 8 K yielding  $a = 2.1$ . The  $T$  dependence of  $H_C$  is shown in the inset by the plot of  $H_C - H_{C0}$  versus  $T$  on double-logarithmic scales, and is also obtained by Quantum Monte Carlo calculations [8]. Right: Schematic view of the phase diagram around the quantum phase transition from a spin-gap to a Néel-ordered ground state at  $H_{C0}$ . The dotted line shows the spin-gap closing due to the Zeeman splitting, and the dashed lines indicate the region of enhanced quantum fluctuations at  $T > 0$ . The thick solid line is the phase boundary  $T_N(H)$  and the thin solid lines indicate the region of enhanced thermal fluctuations.

arrangement of  $\text{Cu}^{2+}$  ions [9]. The main magnetic coupling  $J' \approx 5.5$  meV is present along the rungs, but there are various additional, rather large couplings  $J^0$  present along different other lattice directions [11,12,13,14]. Thus, the magnetic system of  $\text{TlCuCl}_3$  should be viewed as a set of three-dimensionally coupled spin dimers. The inter-dimer couplings  $J^0$  cause a strong dispersion of the triplet excitations, and as a consequence the minimum singlet-triplet gap  $\Delta_m \approx 0.7$  meV is much smaller than  $J$ . A moderate field of about 5 T is already sufficient to close  $\Delta_m$  and induces a Néel order with staggered magnetization perpendicular to the applied field. If there is no magnetic anisotropy in the plane perpendicular to the applied field, this transition is in the same universality class as the Bose-Einstein condensation (BEC) and it is often termed a BEC of magnons. In the zero-temperature limit, it represents an example of a quantum phase transition [15], whose control parameter is the magnetic field strength (see Fig. 1). In the vicinity of a quantum critical point (QCP) anomalous temperature dependencies are expected for various physical properties, as e.g. specific heat  $C$ , susceptibility  $\chi$ , thermal expansion  $\alpha$ , (and resistivity form factors) [16]. In particular, a divergence of the so-called Grüneisen parameter  $\Gamma = C/\alpha$  is expected, when a pressure-dependent QCP is approached [17]. Experimentally, a diverging  $\Gamma(T)$  has indeed been observed for different heavy-fermion compounds [18,19]. Since the phase transition of  $\text{TlCuCl}_3$  is extremely sensitive to pressure [20,21,22,23] and the control parameter may be easily tuned by a variation of the field, this compound is ideally suited to study such generic properties of a QCP.

We present high-resolution measurements of the uniaxial thermal expansion  $\alpha_i = \partial \ln L_i / \partial T$  and the magnetostriction  $\lambda_i = [L_i(H) - L_i(0)] / L_i(0)$  along different lattice di-

rections  $i$  ( $L_i$  is the respective sample length along  $i$ ) as well as specific heat  $C$  and magnetization  $M$  data. The length changes have been measured down to 250 mK by a home-built capacitance dilatometer and  $C$  by a home-built calorimeter for  $T \leq 500$  mK, while the magnetization has been studied by a commercial vibrating sample magnetometer (Quantum Design) for  $T \leq 1.9$  K. All properties have been studied in magnetic fields up to 14 T. Since  $\text{TlCuCl}_3$  easily cleaves along the (010) and (102) planes of the monoclinic structure, we measured  $L_i(H; T)$  perpendicular to these planes on a single crystal of dimensions  $1.7 \times 1.5 \text{ mm}^2$  perpendicular to (010) and (102), respectively. In addition, the [201] direction, which is perpendicular to both other directions, was measured on a second crystal of length  $L_{[201]} = 4.4 \text{ mm}$ . For all three measurement directions the magnetic field was applied along the same direction, namely perpendicular to the (102) plane.

## 2. Results and Discussion

Fig. 2 shows  $\lambda_i$  measured along all three directions for different magnetic fields. In zero field,  $\lambda_i$  has no visible anomalies, but is strongly anisotropic. For  $H \approx 5$  T, pronounced anomalies develop and shift systematically towards higher  $T$  with increasing  $H$ . The  $\lambda_i$  curves for  $i = (010)$  and (102) agree well with our previous results measured on a different crystal for  $T \leq 3$  K [22,24]. The anomalies of  $\lambda_i$  signal large uniaxial pressure dependencies of  $T_N$ , which are related to  $\alpha$  and  $C$  via Ehrenfest's relations

$$\frac{\partial T_N}{\partial p_i} = V_m T_N \frac{\alpha_i}{C} \quad \text{and} \quad \frac{\partial H_C}{\partial p_i} = V_m \frac{\alpha_i}{C} : \quad (1)$$

Here,  $V_m$  is the molar volume and  $\alpha_i$  and  $C$  denote the respective mean-field jumps at  $T_N$ . The second expression of Eq. (1) relates the pressure dependencies of the transition field to the jumps of  $\alpha_i = \partial \lambda_i / \partial H$  and of the differential magnetic susceptibility  $\chi = \partial M / \partial H$ . For  $i = (010)$  and (102), the  $\partial T_N / \partial p_i$  largely cancel each other under hydrostatic pressure, since the anomalies are of comparable magnitudes but of opposite signs. Thus, the hydrostatic pressure dependence  $\partial T_N / \partial p_{\text{hydro}}$  is essentially determined by the sign and size of the anomaly of  $\lambda_{201}$ . Obviously, the anomalies of  $\lambda_{201}$  are the largest ones and their positive signs mean that  $T_N$  drastically increases for uniaxial pressure along [201] as well as for hydrostatic pressure. Fig. 3 shows the field derivatives of the magnetostriction. A gain, we find the characteristic anisotropy that the anomalies of  $\lambda_{010}$  and  $\lambda_{102}$  are of similar sizes but opposite signs, while significantly larger anomalies are present for  $\lambda_{201}$ . Thus, the hydrostatic pressure dependence of  $H_C$  is again essentially identical to that for uniaxial pressure along [201].

In Ref. [22] we have shown that the pressure dependencies of  $T_N$ ,  $H_C$ , and the magnetic susceptibility in the paramagnetic phase can be traced back to the pressure-dependent changes of a single parameter, which in the case of  $\text{TlCuCl}_3$  is the intra-dimer coupling  $J$ . This conclusion was based on the measurements perpendicular to the (010) and (102)

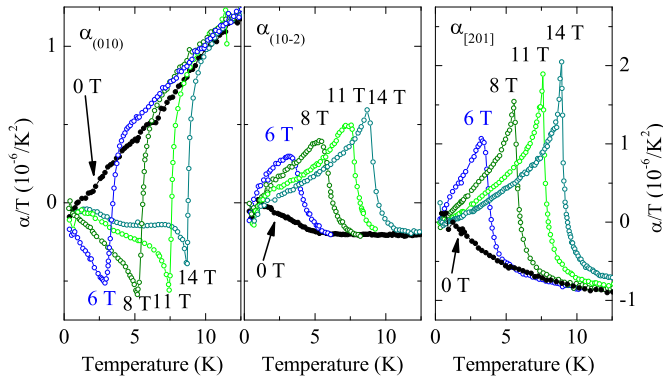


Fig. 2. Thermomagnetic expansion along different directions for various magnetic fields applied perpendicular to the (102) cleavage plane of  $\text{TlCuCl}_3$ . Note the different scale for the [201] direction.

planes, and is fully confirmed by the additional new data along the [201] direction. From the zero-temperature extrapolations of the uniaxial pressure dependencies of  $H_c$  for  $i = (010)$  and  $(102)$  we estimated  $\partial \ln H_c = \partial p_i / + 190\% / \text{GPa}$  and  $\partial \ln H_c = \partial p_i / + 180\% / \text{GPa}$ . Since the anomalies for the [201] direction are about twice as large, we obtain  $\partial \ln H_c = \partial p_i / + 370\% / \text{GPa}$  for pressure along [201] and  $\partial \ln H_c = \partial p_{\text{hydro}} / + 360\% / \text{GPa}$  for hydrostatic pressure. The latter value is in reasonable agreement with direct measurements under hydrostatic pressure, which yield  $\partial \ln H_c = \partial p_{\text{hydro}} / + 400\% / \text{GPa}$  for the initial slope at ambient pressure [23].

The shape of the  $\lambda_i$  anomalies is typical for a second-order phase transition with a pronounced mean-field contribution causing a jump at  $T_N$ , superimposed by fluctuations causing a divergence  $\lambda_i / T$  with the reduced temperature  $t = (T - T_N) / T_N$  and the critical exponents depending on the universality class of the phase transition. On approaching  $H_{c0} = H_c(T \rightarrow 0) / 4.8 \text{ T}$ , the  $\lambda_i$  anomalies broaden to some extent (see below). The  $\lambda_i$  anomalies also show a pronounced fluctuation contribution for  $T > 2 \text{ K}$ , but become more jump-like for lower  $T$ . The changing shapes of both, the  $\lambda_i$  and the  $\lambda_{\text{total}}$  anomalies can be intuitively understood from Fig. 1, because (i) the absolute temperature region around the phase boundary where fluctuations become important decreases with decreasing  $T_N$ , and (ii) close to  $H_{c0}$  the phase boundary is crossed with a very small slope as a function of  $T$ , so that the fact that  $H_c$  is not infinitely sharp becomes more and more important. As a criterion for  $H_c$ , we used the maximum of the second derivatives  $\partial^2 \lambda_i = \partial H^2$ , whose full widths at half maximum amount to  $\approx 0.45 \text{ T}$  (see Inset of Fig. 3). We suspect that this width mainly arises from internal stresses, which broaden the transition due to the strong (uniaxial) pressure dependencies of  $H_c$ . We have also investigated, whether there is a finite hysteresis of  $H_c$  by measuring  $\lambda_i(H)$  with increasing and decreasing  $H$ . For a drift rate of  $0.1 \text{ T/m}$  in we obtain a difference  $H_c^{\text{up}} - H_c^{\text{down}} \approx 0.04 \text{ T}$ , which does hardly change with temperature. At  $T = 0.3 \text{ K}$  we also measured with  $0.01 \text{ T/m}$  in and found  $H_c^{\text{up}} - H_c^{\text{down}} \approx 0.01 \text{ T}$ , i.e., the observed hysteresis partly arises from the finite field drift. Thus, we regard the phase transition as

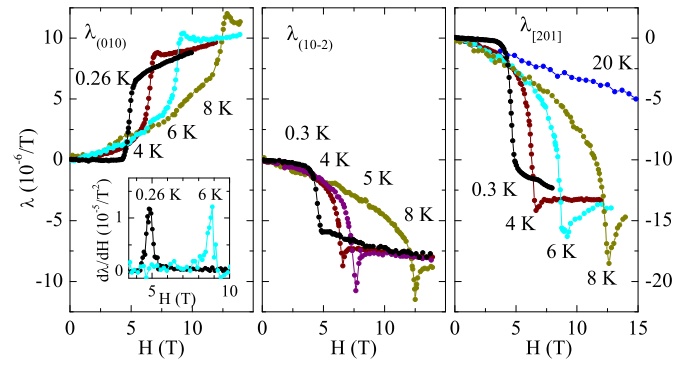


Fig. 3. Magnetostriction coefficient  $\lambda_i$  at  $\lambda_i = dH$  measured along different directions  $i$  at various temperatures. In all cases the magnetic field has been applied perpendicular to the (102) plane (see text).

a second-order one with a weak first-order contribution. The first-order contribution most probably arises from the large spin-lattice coupling, which may drive a second-order into a first-order transition [25]. It is also possible that a transition transforms from second to first order, when  $T_c$  is suppressed towards 0 K by an external parameter. However, the weak temperature-dependence of the hysteresis observed in  $\text{TlCuCl}_3$  does not give any evidence for such a scenario, and we suspect that the transition of  $\text{TlCuCl}_3$  remains (almost) continuous down to lowest  $T$ .

As mentioned above, a diverging Grüneisen parameter ( $\Gamma \rightarrow 0$ ) has been predicted at  $H = H_{c0}$  [17]. Before comparing our experimental data to this prediction, we will discuss from a phenomenological point of view what may be expected for when the QCP is approached along different routes in the phase diagram. Using Maxwell's relations one finds that  $\lambda_i = \partial S = \partial p$ , while  $C = T = \partial S = \partial T$ . If a thermodynamic system can be described by a single energy scale  $E$ , its entropy  $S$  only depends on the ratio  $T = E$ , i.e.  $S(T; E) = S(T = E)$  with a model-dependent function  $S(x)$ . Comparing the  $T$ - and  $p$ -derivatives of  $S(T = E(p))$  yields the Grüneisen scaling

$$\Gamma = \frac{\lambda_i(T)}{C(T)} = \frac{\partial \ln E}{\partial p}; \quad (2)$$

which is temperature independent. Prominent examples of such systems are the Debye model with  $E = E_D$ , the almost free electron gas with  $E = E_F$ , or magnetically ordered states with exchange coupling  $J = E$  (for  $T \ll T_c$ ). In real systems, one usually observes a weakly  $T$ -dependent  $\Gamma(T)$ , which is due to the fact that the above-mentioned single-parameter models only consider the leading energy scale and neglect others. If several energy scales  $E_i$  are equally important, the individual  $E_i$  usually have different pressure dependencies, and therefore the  $p$ - and  $T$ -derivatives are, in general, not (almost) proportional to each other. However, it is possible that for different temperature regions different  $E_i$ 's are dominant and in the respective regions  $\Gamma = \partial \ln E_i = \partial p$  holds. An example is a coupled spin-dimer system as it is realized in  $\text{TlCuCl}_3$ . For high temperatures ( $T \gg J; J^0$ ), the behavior is determined by the average

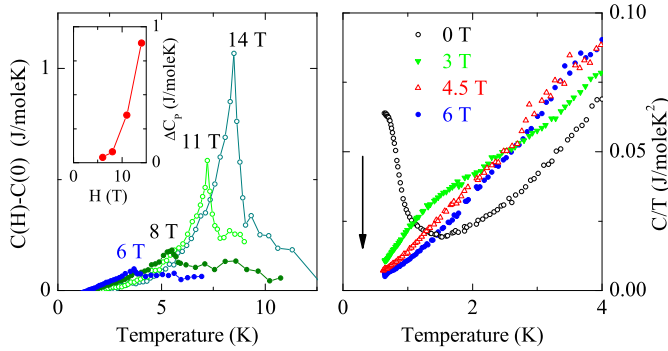


Fig. 4. Left: Difference of the specific heat  $C$  in finite and zero magnetic field. The inset shows the anomaly heights as a function of field. Right: Expanded view of the low-temperature  $C = T$  for different fields below and above the critical field  $H_{C0} \approx 4.8$  T. The arrow indicates increasing magnetic field strength. (see text)

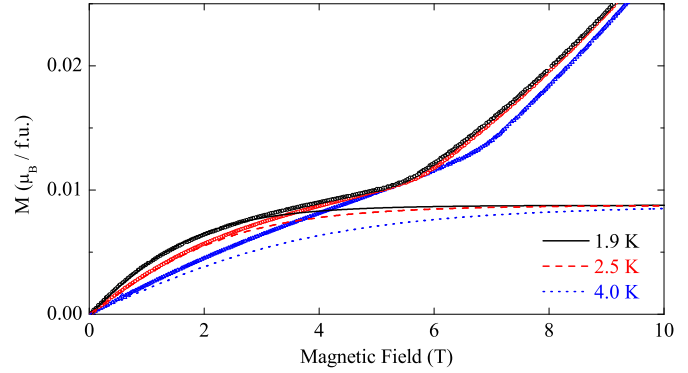


Fig. 5. Magnetization (symbols) of  $TlCuCl_3$  at different temperatures. The finite magnetization in the gap region can be well reproduced by Brillouin functions (lines) assuming magnetic impurities with spin  $S = 1$ . (see text)

spin gap  $\hbar\omega$ , while the minimum gap  $\omega_m$  becomes dominant at  $T_m$ . Thus,  $\langle T \rangle$  varies from  $\langle T \rangle_{m=0} = \langle T \rangle_{\omega_m=0}$  to  $\langle T \rangle_{m=\omega_m}$  with increasing  $T$ . In  $TlCuCl_3$ , the zero-field gap  $\omega_m \approx 8$  K linearly decreases with  $H$  [13], i.e.  $\omega_m(H) = \omega_m^0 - h$  where  $h = gH = k_B T$ ,  $g$  is the  $g$ -factor and  $k_B$  Boltzmann's constant. Thus, at a given field  $H < H_{C0}$  the temperature, below which  $\omega_m$  is expected to approach a constant, decreases with  $H$ . For  $H \rightarrow H_{C0}$ , however,  $\langle T \rangle_m \propto \frac{1}{\omega_m} \frac{\partial \omega_m}{\partial p}$  diverges, because  $\omega_m \rightarrow 0$ .

For  $H > H_{C0}$ , i.e. in the ordered phase, the characteristic low-temperature energy scale is given by the spin wave velocity  $v$ . To our knowledge, the exact dependence of  $v$  on  $H < H_{C0}$  is not known, but it is quite natural that  $v$  disappears when  $H_{C0}$  is approached. For simplicity, we assume  $v \propto (H - H_{C0})^n$  with  $n > 0$  and derive  $\langle T \rangle_m \propto \langle T \rangle_{v=0} \propto \frac{1}{v} \frac{\partial v}{\partial p} \propto \frac{1}{H - H_{C0}} \frac{\partial H_{C0}}{\partial p}$ . Thus, the Grüneisen parameter is again expected to approach a constant, which diverges for  $H \rightarrow H_{C0}$ , but the sign of the divergence for  $H > H_{C0}$  is opposite to that for  $H < H_{C0}$ .

In a next step we will approach the QCP along the phase boundary  $T_N(H)$  for  $H > H_{C0}$ . For clarity, we use the approximation  $T_N(H) = b(H - H_{C0})^\nu$  with  $\nu = 1 = 2 = 3$  for  $H \rightarrow H_{C0}$  (see Fig. 1 and Refs. [8,26]), and calculate  $\langle T_N \rangle = \langle T \rangle_p = \nu b (H - H_{C0})^{\nu-1} \langle T \rangle_{H_0=0}$ . Obviously,  $\langle T_N \rangle = \langle T \rangle_p$  diverges for  $H \rightarrow H_{C0}$  for  $\nu < 1$ , and the sign of this divergence is opposite to the sign of  $\partial H_{C0} / \partial p$ . We emphasize that this result follows from the finite slope of the phase boundary for  $H \rightarrow H_{C0}$ , and does not depend on the particular choice of  $T_N(H)$ . Since the pressure dependence of  $T_N$  is given by Ehrenfest's relation (1), the ratio  $\langle T \rangle = C$  of the thermal expansion and specific-heat anomalies at  $T_N$  is expected to diverge for  $H \rightarrow H_{C0}$ . From Eq. (1), it is also clear that the vanishing  $T_N$  would cause a divergence of  $\langle T \rangle = C$  even if the slope of the phase boundary was finite and  $\partial T_N / \partial p$  would thus not diverge for  $H \rightarrow H_{C0}$ .

Let us summarize the above considerations. On approaching  $H_{C0}$  we expect (i) for  $H < H_{C0}$  that  $\langle T \rangle(H) \propto \langle T \rangle_{\omega_m=0}$ , which diverges for  $H \rightarrow H_{C0}$ , (ii) for  $H > H_{C0}$  a similar divergence of  $\langle T \rangle_m \propto \langle T \rangle_{v=0}$ , but of the

opposite sign, and (iii) a divergence of the ratio  $\langle T \rangle = C$ , which has the same (opposite) sign as the divergence of  $\langle T \rangle$  above (below)  $H_{C0}$ . Since the above considerations are rather general, one may expect a divergence of  $\langle T \rangle$  close to many kinds of transitions, whose  $T_c$  is suppressed to 0 K. To obtain more information about a quantum phase transition, one has to consider the actual temperature dependencies  $\langle T \rangle$ ,  $C(T)$ , and/or  $\langle T \rangle$ , as it has been done e.g. by the authors of Refs. [17,27,28].

In Fig. 4 we show the specific heat anomalies for different magnetic fields. In agreement with Ref. [29] we find rather small anomalies even for the largest field, and their magnitude rapidly decreases when  $H_{C0}$  is approached (see Inset of Fig. 4). Since the magnitude of the respective  $\Delta C_p$  anomalies changes much less with field (see Fig. 2), the expected divergence of  $\partial T_N / \partial p$  for  $H \rightarrow H_{C0}$  is obviously confirmed by the experimental data, since the denominator in Eq. (1) vanishes. This is the case for all three directions of uniaxial as well as for hydrostatic pressure. In the right panel of Fig. 4 we show an expanded view of the low-temperature behavior of some  $C(T; H) = T$  curves. For zero field, the onset of an anomaly can be clearly seen [30], and this anomaly is suppressed above about 3 T. We suspect that this anomaly arises from an ordering of magnetic impurities. The presence of such impurities is also evident from the finite magnetization in the gap region  $H < H_{C0}$  at low  $T$ , which can be well reproduced by Brillouin functions (see Fig. 5). The corresponding fits of the data at  $T = 1.9$  K and 2.5 K yield 0.4% of magnetic impurities with spin  $S = 1$ . The Brillouin function calculated for the same parameters and  $T = 4$  K is somewhat smaller than the experimental data for  $H \approx 1$  T. This is expected, because at this higher temperature a sizeable magnetization from excited triplets is already present. Probably, the  $S = 1$  impurities are mostly ferromagnetically aligned spin dimers, because the intra-dimer coupling between the spin-1/2  $Cu^{2+}$  ions arises from a  $\approx 96\%$  superexchange via the  $p$  orbitals of the  $Cl$  ions, which is very sensitive to changes in the bond angle. The impurities strongly influence the low-temperature behavior of  $C(T)$  for low fields, but become much less in-

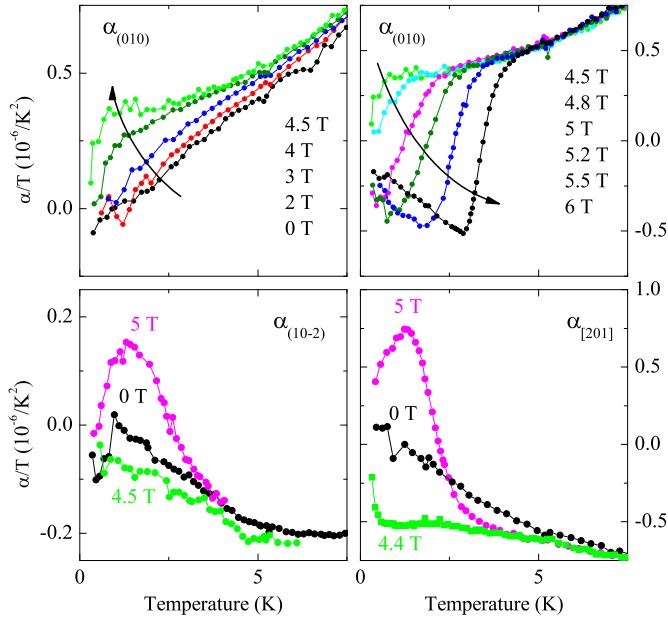


Fig. 6. Top: Thermal expansion perpendicular to the (010) plane for different magnetic fields below (left) and above (right) the critical field. The arrows indicate increasing magnetic-field strength. The bottom panels show some  $\alpha_i(T)$  curves for the other directions.

ential at higher fields because the moments are almost completely saturated for  $H \geq 3$  T and  $T \leq 2$  K. It is, however, unclear to what extent the impurities may change the (critical) behavior close to the phase transition.

Fig. 6 shows an expanded view of the low- $T$  behavior of  $\alpha_i(T)$ . In zero field,  $\alpha_i(T)$  continuously approaches zero for  $T \rightarrow 0$ , while for larger  $H$  it shows a pronounced shoulder, which systematically increases and reaches a maximum slightly below  $H_{C0}$ . For larger fields clear anomalies with a sign change of  $\alpha_i(T)$  occur, and these anomalies systematically sharpen with further increasing field. The behavior is essentially the same for all three directions, only the magnitudes and signs are different [31]. As already mentioned, we attribute the broadening of the anomalies when  $H_{C0}$  is approached from larger fields to the finite width of the phase transition. This also explains that the  $\alpha_i(T)$  curves show anomalies already for  $H \geq 4.6$  T, i.e. below  $H_{C0} \approx 4.8$  T determined by the magnetostriction measurements.

In Fig. 7 we present  $\alpha_i$  for different magnetic fields. For all three directions  $\alpha_i$  shows the tendency to diverge with decreasing  $T$  for  $H \geq 4.5$  T. For lower  $H$ , the  $\alpha_i(T)$  follow the same curve at higher  $T$ , but seem to approach finite values for  $T \rightarrow 0$ . The magnitudes of these limiting values increase with increasing field and the temperature, below which the deviation sets in, decreases. The  $\alpha_i(T)$  for  $H > H_{C0}$  also follow the general curve at higher  $T$ , until a large anomaly signals the crossing of the phase boundary. For all three directions, the magnitudes of these anomalies drastically increase with decreasing  $H$  and the signs are opposite to the respective signs of the diverging  $\alpha_i(T)$  for  $H < H_{C0}$ .

On this qualitative level, our experimental data of  $\alpha_i(T)$  very well confirm the behavior, which one can expect from

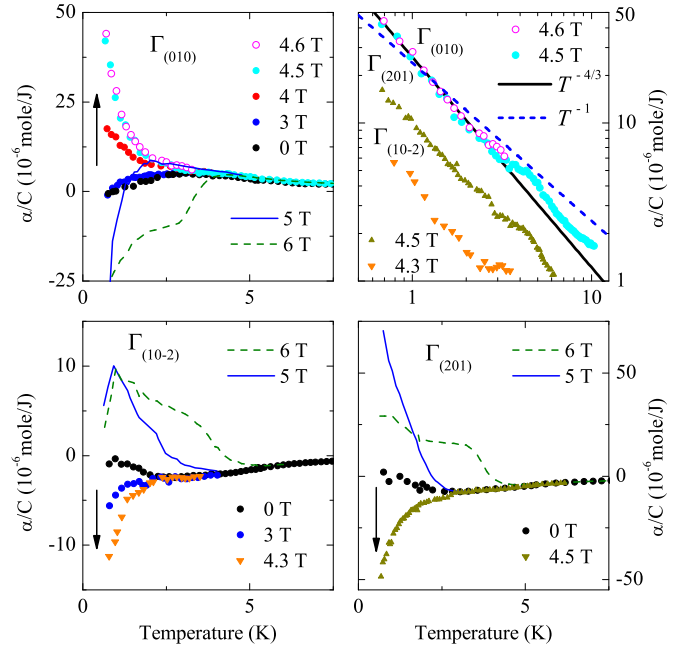


Fig. 7. Grüneisen parameters  $\alpha_i$  obtained from the thermal expansion along different measurement directions  $i$  in magnetic fields below (symbols, increasing field strength is indicated by the arrows) and above (lines) the QCP at  $H_{C0} \approx 4.8$  T. The upper right panel shows  $\alpha_i(T)$  for  $H \geq H_{C0}$  on double-logarithmic scales. Here, the negative  $\alpha_i(T)$  for  $i = (10\bar{2})$  and  $[201]$  have been divided by a factor of 2 and 3, respectively. The solid line is a power-law fit of  $\alpha_{010}$  yielding  $1=T^{-4/3}$  and, for comparison, the expected  $1=T$  behavior is shown by the dashed line (see text).

the above considerations of the gap closing for  $H < H_{C0}$  and the shape of the phase boundary for  $H > H_{C0}$ . For a deeper understanding, one has to compare the experimental data quantitatively to theoretical predictions. According to Ref. [17] the following temperature dependencies are expected  $H = H_{C0}$ :

$$C = T / T^p; \quad \alpha = T / 1 = T^p, \quad \text{and} \quad \alpha / 1 = T^p \quad (3)$$

In the upper right panel of Fig. 7 we show the diverging  $\alpha_i(T)$  for  $H \geq H_{C0}$  on double-logarithmic scales. Because of the negative signs,  $\alpha_{10\bar{2}}$  and  $\alpha_{201}$  have been divided by the factors 2 and 3, respectively. Apparently, the slope is the same within experimental accuracy. The solid line is a power-law fit of  $\alpha_{010}$  which yields  $T^{-4/3}$  and describes the experimental data reasonably well for about one decade. For comparison, the predicted  $1=T$  behavior is also shown (dashed line). In view of the fact that the theoretical prediction only considers the irregular contributions of  $C$  and  $\alpha_i$ , while the experimental data also contain the phononic contributions of  $C$  and  $\alpha_i$ , one may tend to the conclusion that our data nicely confirm the theoretical prediction for  $\alpha_i(T)$ . However, the agreement between theory and experiment becomes much worse when the individual temperature dependencies of  $C = T$  and  $\alpha_i = T$  are considered. Neither the data of Fig. 4 nor those of Fig. 6 give any indication to follow the predicted temperature dependencies of Eq. (3). Concerning the specific heat data, one might

argue that the predicted  $\chi^{-1}$  behavior is difficult to identify because of the phononic contribution and the influence of the magnetic impurities. This argument is less convincing for  $\chi^{-1}(T) \sim T$ , since (i) the predicted divergence should be seen despite a (regular) phononic contribution and (ii) the ordering of the magnetic impurities does not cause a sizeable anomaly in the zero-field data [31]. Thus, we conclude that our present experimental data of  $\text{TCuCl}_3$  do not confirm the theoretical predictions [17]. However, our data do not disprove the theoretical predictions either. Experimentally, one can suspect that in order to observe the predicted temperature dependencies it would be necessary to study (i) samples with significantly reduced transition widths and less magnetic impurities, and (ii) it might be necessary to extend the measurements to lower temperatures. Moreover, the theoretical predictions have been calculated for clean and isotropic systems. It is not clear to what extent the temperature dependencies of  $\chi$  and  $C$  are influenced by disorder or a finite magnetic anisotropy. The latter is reflected in the  $\sim 10\%$  anisotropy of the  $g$  factors of  $\text{TCuCl}_3$  for different magnetic field orientations [32].

### 3. Summary

In summary, we have presented high-resolution measurements of the magnetic expansion and magnetostriction along different lattice directions of  $\text{TCuCl}_3$ . Both quantities show very pronounced and strongly anisotropic anomalies at the phase boundary of the field-induced Néel order  $T_N(H)$  for  $H > H_{C0}$ , and signal very large and strongly anisotropic uniaxial pressure dependencies of the transition temperatures and fields. The hydrostatic pressure dependence of the spin gap  $\Delta_m$  for  $H \ll H_{C0}$  obtained from our data using Ehrenfest's relations is in reasonable agreement with the value observed by direct measurements under hydrostatic pressure. In addition, our data confirm the diverging pressure dependencies  $\partial T_N / \partial p_i$  for  $H \ll H_{C0}$ , which are expected from the finite slope  $\partial T_N / \partial H$  of the phase boundary for  $H \ll H_{C0}$ , i.e. when the quantum critical point is approached. For  $H < H_{C0}$ , the Grüneisen parameters  $\gamma_i = \alpha_i / C$  are expected to approach constant values for  $T \ll T_N(H)$ , which diverge for  $H \ll H_{C0}$ , and  $\chi^{-1}(T) / T$  has been predicted at  $H = H_{C0}$ . In fact, the experimental  $\chi^{-1}(T)$  for all three measurement directions are in qualitative agreement with these expectations. However, the temperature dependencies predicted for the individual quantities  $\chi^{-1}(T)$  and  $C(T)$  are not observed experimentally. For  $H \ll H_{C0}$  the low- $T$  behavior of both  $\chi^{-1}$  and  $C$  is influenced by the finite transition width and for lower fields at least  $C(T)$  is also affected by the presence of magnetic impurities. Thus, future measurements on samples of improved quality as well as calculations considering the influence of disorder and weak magnetic anisotropy may clarify the reasons for the puzzling temperature dependencies of  $\chi^{-1}(T)$ ,  $C(T)$ , and  $\chi^{-1}(T)$ .

We acknowledge fruitful discussions with A. Rosch, I. Fischer, and J.A. Mydosh. This work was supported

by the Deutsche Forschungsgemeinschaft via Sonderforschungsbereich 608.

### References

- [1] P. Lemmens, G. Güntherodt, and C. Gros. Phys. Rep. 375, 1 (2003).
- [2] G.S. Uhrig and H.J. Schulz. Phys. Rev. B 54, 9624 (1996).
- [3] E. Dagotto and T.M. Rice. Science 271, 618 (1996).
- [4] B.S. Shastry and B. Sutherland. Physica B 108, 1069 (1981).
- [5] M. Hase, I. Terasaki, and K. Uchinokura. Phys. Rev. Lett. 70, 3651 (1993).
- [6] E. Dagotto. Rep. Prog. Phys. 62, 1525 (1999).
- [7] H. Kageyama, K. Yoshimura, R. Stern, N.V. Mushnikov, K. Onizuka, M. Kato, K. Kosuge, C.P. Slichter, T. Goto, and Y. Ueda. Phys. Rev. Lett. 82, 3168 (1999).
- [8] O. Nohadani, S. Wessel, B. Normand, and S. Haas. Phys. Rev. B 69, 220402(R) (2004).
- [9] H. Tanaka, A. Osawa, T. Kato, H. Uekusa, Y. Ohashi, K. Kakurai, and A. Hoser. J. Phys. Soc. Japan 70 (4), 939 (2001).
- [10] A. Osawa, T. Takamasu, K. Tatani, H. Abe, N. Tsuji, O. Suzuki, H. Tanaka, G. Kido, and K. Kondo. Phys. Rev. B 66 (2002).
- [11] T. Nikuni, M. Oshikawa, A. Osawa, and H. Tanaka. Phys. Rev. Lett. 84, 5868– (2002).
- [12] M. Matsumoto, B. Normand, T.M. Rice, and M. Sigrist. Phys. Rev. Lett. 89 (2002).
- [13] Ch. Ruegg, N. Cavadini, and A. Furrer. Nature 423, 62 (2003).
- [14] M. Matsumoto, B. Normand, T.M. Rice, and M. Sigrist. Phys. Rev. B 69, 054423 (2004).
- [15] M. Vojta. Rep. Prog. Phys. 66, 2069 (2003).
- [16] G.R. Stewart. Rev. Mod. Phys. 73, 797 (2001).
- [17] L. Zhu, M. Garst, A. Rosch, and Q. Si. Phys. Rev. Lett. 91, 066404 (2003).
- [18] R. Kuchler, N. Oeschler, P. Gegenwart, T. Cichorek, K. Neumaier, O. Tegus, C. Geibel, J.A. Mydosh, F. Steglich, L. Zhu, and Q. Si. Phys. Rev. Lett. 91, 066405 (2003).
- [19] R. Kuchler, P. Gegenwart, K. Heuser, E.-W. Scheidt, G.R. Stewart, and F. Steglich. Phys. Rev. Lett. 93, 096402 (2004).
- [20] A. Osawa, M. Fujisawa, T. Osakabe, K. Kakurai, and H. Tanaka. J. Phys. Soc. Japan 72, 1026 (2003).
- [21] H. Tanaka, K. Goto, M. Fujisawa, T. Ono, and Y. Uwatoko. Physica B 329, 697 (2003).
- [22] N. Johansson, A. Vasiliev, A. Osawa, H. Tanaka, and T. Lorenz. Phys. Rev. Lett. 95, 017205 (2005).
- [23] K. Goto, T. Ono, H. Tanaka, and Y. Uwatoko. Prog. Theor. Phys. Suppl. 159, 397 (2005).
- [24] N. Johansson, A. Osawa, H. Tanaka, A. Vasiliev, and T. Lorenz. Physica B (in press; cond-mat/0504383).
- [25] K.K. Murata. Phys. Rev. B 15, 4328 (1977).
- [26] S. Wessel, M. Oshani, and S. Haas. Phys. Rev. Lett. 87 (2001).
- [27] M. Garst and A. Rosch. Phys. Rev. B 72, 205129 (2005).
- [28] I. Fischer and A. Rosch. Phys. Rev. B 71, 184429 (2005).
- [29] A. Osawa, H. A. Katori, and H. Tanaka. Phys. Rev. B 63 (2001).
- [30] Such an anomaly is not seen in Ref. [29], where  $C(T)$  versus  $T$  is plotted for  $T \leq 1$  K. Plotting in the same representation and temperature range, this anomaly is not visible in our data, too.
- [31] In zero field there is a small anomaly in  $\chi^{-1} \sim T$  around 1 K. At present its origin is unclear, it might be related to the anomaly observed in  $C \sim T$  for zero field.
- [32] V.N. Glazkov, A.I. Smimov, H. Tanaka, and A. Osawa. Phys. Rev. B 69, 184410 (2004).